

SZCZEGÓLNE PRZYPADKI STYKU WEWNĘTRZNEGO ELEMENTÓW CYLINDRYCZNYCH O PORÓWNYWALNYCH ŚREDNICACH

PARTICULAR CASES OF INNER CONTACT CYLINDERS HAVING COMPARABLE DIAMETERS

W artykule podjęto problem styku wewnętrznego elementów cylindrycznych o porównywalnych średnicach z małymi odchyłkami od kształtu kołowego. Przedstawiono wyniki przybliżonego rozwiązania równania podstawowego opisującego styk dwuobszarowy, oraz rozważano współpracę elementów z błędami owalności oraz graniastości potrójnej i poczwórnej. Rozwiązania numeryczne przedstawione zostały w postaci wykresów.

Wszystkie znane badania dotyczące współpracy elementów cylindrycznych nie uwzględniają w swoich rozwiązaniach wpływu małych odchyłek od kształtu kołowego takich np. jak eliptyczność, owalność i graniastość. Odchyłki te mają istotny wpływ na wielkość i rozkład nacisków stykowych. Ich ocena ilościowa ma duże znaczenie praktyczne.

Słowa kluczowe: elementy cylindryczne, styk dwuobszarowy, eliptyczność, owalność

The paper presented inner contact of cylinders having comparable in case of small out-of-roundness. There are presented results of asymptotic solutions, by collocation method the basic equation describing contact problem. The particular cases contact problem and deviations from circular shape, like bi-ared contact and joints with lobing elements were carried out. Numerical calculation were presented in graphical way.

All well-known solutions of cylindrical joints do not take into account small deviations from circular shape, like ellipticity, lobing, ovality and so forth. The deviation of element contours has an effect on magnitude and distribution of the contact pressures. Therefore quantitative estimation of the effect is very important for practical reasons.

Keywords: mechanical contact, cylindrical elements, bi-area contact, lobing elements

1. Introduction

All well-known solutions of cylindrical joints do not take into account small deviations from circular shape, like ellipticity, lobing, ovality and so forth. The deviation of element contours has an effect on magnitude and distribution of the contact pressures. Therefore quantitative estimation of the effect is very important for practical reasons. In the presented article, authors' original results were presented. Quotation of earlier known solutions [1, 2, 3] were limited to indispensable minimum.

2. Basic equation of the problem

Interaction of the elements, of contours L_1 and L_2 (Fig. 1), in contact is caused by static forces N , T and couple of forces having moment M_0 . Problem consists on determining distribution pressures contact $p(\alpha, \delta)$ and the contact zone limited by the angles $\alpha_{0\delta}$ and $\beta_{0\delta}$.

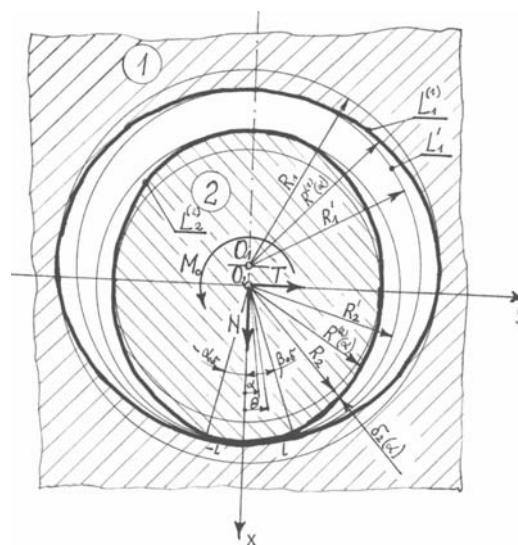


Fig.1. Scheme of the cylindrical joint for elements with small out-of-roundness

Equation obtained for $p(\alpha, \delta)$ in [3] takes the form:

$$\begin{aligned}
 k_1 \int_{-\alpha_{os}}^{\beta_{os}} ctg \frac{\alpha - \theta}{2} [p'(\theta, \delta) + fp(\theta, \delta)] d\theta &= k_2 [p(\alpha, \delta) - fp'(\alpha, \delta)] + \\
 + k_3 \int_{-\alpha_{os}}^{\beta_{os}} p(\alpha, \delta) d\alpha + k_4 (N \cos \alpha + T \sin \alpha) + \frac{R_1 - R_2}{R_1 R_2} - & \quad (1) \\
 -sin\pm \left\{ 2 \left[\frac{f'_{1x}(\pm)}{R_1^2} - \frac{f'_{2x}(\pm)}{R_2^2} \right] - \left[\frac{f''_{1y}(\pm)}{R_1^2} - \frac{f''_{2y}(\pm)}{R_2^2} \right] \right\} + cos\pm \left\{ 2 \left[\frac{f'_{1y}(\pm)}{R_1^2} - \frac{f'_{2y}(\pm)}{R_2^2} \right] + \left[\frac{f''_{1x}(\pm)}{R_1^2} - \frac{f''_{2x}(\pm)}{R_2^2} \right] \right\}
 \end{aligned}$$

where: $f_{kx}(\alpha), f_{ky}(\alpha)$ - parameters describing deviation of contour L_1 (hole, $k=1$) and L_2 (disk, $k=2$) from given principal circles; $f_{kx}(\alpha) = x_k^*(\alpha, \delta) - x_k(\alpha), f_{ky}(\alpha) = y_k^*(\alpha, \delta) - y_k(\alpha), x_k^*, y_k^*$ - parametric equations of elements out - for displacements of round contours before strain.

$$\begin{aligned}
 k_1 &= \frac{I}{8\pi} \left(\frac{1 + \kappa_1}{G_1 R_1} + \frac{1 + \kappa_2}{G_2 R_2} \right) \\
 k_2 &= -\frac{I}{4} \left(\frac{1 - \kappa_1}{G_1 R_1} - \frac{1 - \kappa_2}{G_2 R_2} \right) \\
 k_3 &= \frac{I + k_1}{8\pi G R} \\
 k_4 &= \frac{I}{2\pi} \left(\frac{\kappa_1}{G_1 R_1} + \frac{1}{G_2 R_2} \right)
 \end{aligned}$$

G - shear modulus, $\kappa = 3 - 4\nu$ - for plane state of strain, $\kappa = (3 - \nu)/(1 + \nu)$ - for plane state of stress, ν - Poisson ratio,

$$p'(\theta, \delta) = dp(\theta, \delta) / d\theta;$$

$$\begin{aligned}
 \begin{Bmatrix} N \\ T \end{Bmatrix} &= - \int_{-\alpha_{os}}^{\beta_{os}} \left[\sigma_r^{(2)}(\alpha, \delta) \begin{Bmatrix} \cos \alpha \\ \sin \alpha \end{Bmatrix} + m \tau_{ra}^{(2)}(\alpha, \delta) \begin{Bmatrix} \sin \alpha \\ \cos \alpha \end{Bmatrix} \right] d\alpha \\
 \delta_r(\alpha, \delta) &= -p(\alpha, \delta) \\
 \tau_{ra}(\alpha, \delta) &= f \delta_r(\alpha, \delta)
 \end{aligned}$$

f - coefficient of sliding friction.

3. Bi-area contact of cylinders with ellipticity

We assume that elements are made of the same material ($G_1 = G_2 = G, \nu_1 = \nu_2$) and in the contact zone $f = 0$. Contact mating of elements in the joint is determined only by force N , hence $\alpha_{os} = \beta_{os}$. Semi-axes of elliptic elements (Fig. 1) are equal:

$$\begin{aligned}
 a_1 = R_1, \quad b_1 = R_1, \quad a_2 = R_2, \quad b_2 = R_2 \\
 \text{and } a_1 > b_1, \quad a_2 > b_2
 \end{aligned}$$

Elements radii are similar, i.e. $R_1 \approx R_2 = R$, but radial clearance $\varepsilon = R_1 - R_2 > 0$.

Particular cases of cylinder deviations of their joints, two areas of contact may appear. Fig. 2 shows such a case with symmetric distribution of contact areas S_1 and S_2 in relation to pressing force N . Contact of the disk 2 with the hole 1 at first takes place in points P_1 and P_2 situated under the angle 2λ .

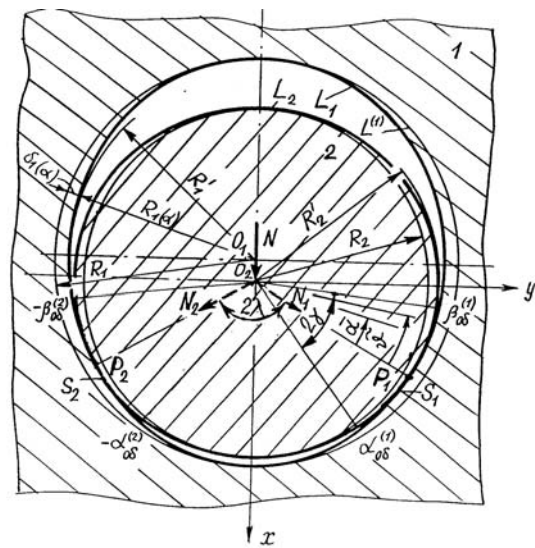


Fig. 2. Scheme of bi-area contact in the cylindrical joint

Calculations of the contact pressures and their distribution in the contact zones $S_1 (\alpha_{os}^{(1)} \leq \alpha \leq \beta_{os}^{(1)})$ or $S_2 (-\alpha_{os}^{(2)} \leq \alpha \leq -\beta_{os}^{(2)})$ are carried out according to (1), where the limits of integration correspond with the limits of contact zones, and N is substituted by $N' = 0,5N / \cos \lambda$. An angle λ is determined from cotangency condition of element contours 1 and 2 points P_1 and P_2 . In the case of ellipses, in co-ordinates xOy , these conditions take the form:

$$\left. \begin{aligned}
 \frac{(x_o + D)^2}{a_1^2} + \frac{y_o^2}{b_1^2} &= 1 \\
 \frac{x_o^2}{b_2^2} + \frac{y_o^2}{a_2^2} &= 1
 \end{aligned} \right\} \quad (2)$$

$$\frac{b_1^2}{a_1^2} (x_o + \Delta) = \frac{a_2^2}{b_2^2} x_o \quad (3)$$

where: Δ - distance between points O_1 and O_2, x_o, y_o - co-ordinates of contact point of contours.

Quantities Δ, x_o, y_o are expressed by equations:

$$x_o = \frac{b_1 b_2^2}{a_2} \sqrt{\frac{b_1^2 - a_2^2}{a_1^2 a_2^2 - b_1^2 b_2^2}} \quad (4)$$

$$y_o = \pm \sqrt{\frac{a_1^2 a_2^4 - b_1^4 b_2^2}{a_1^2 a_2^2 - b_1^2 b_2^2}}$$

After transformations we obtain:

$$\lambda = \arctg \frac{a_2}{b_1 b_2^2} \sqrt{\frac{a_1^2 a_2^4 - b_1^2 b_1^4}{b_1^2 - a_2^2}} \quad (5)$$

In considered case, there possible cases of bi-area contact are possible:

- 1) elements 1 and 2 are elliptic,
- 2) element 1 is elliptic and element 2 is circular,
- 3) element 1 is circular and element 2 is elliptic.

Equation for the contact pressures $p(\tilde{\alpha}, \delta)$ takes the form:

$$\frac{1}{\pi} \int_{\gamma_1}^{\gamma_2} \text{ctg} \frac{\tilde{\alpha} - \tilde{\theta}}{2} p'(\tilde{\theta}, \delta) d\tilde{\theta} = \frac{2}{\pi} \cos \tilde{\alpha} \int_{\gamma_1}^{\gamma_2} p(\tilde{\alpha}, \delta) \cos \tilde{\alpha} d\tilde{\alpha} + \quad (6)$$

$$+ \frac{1}{2\pi} \int_{\gamma_1}^{\gamma_2} p(\tilde{\alpha}, \delta) d\tilde{\alpha} + \frac{4\varepsilon G}{R(1+\chi)} \left[1 - \frac{\varepsilon_1}{\varepsilon} D_1(\alpha) - \frac{\varepsilon_2}{\varepsilon} D_2(\alpha) \right]$$

where: $\tilde{\alpha} = \alpha + \lambda, 0 \leq \alpha \leq \frac{\pi}{2}, \tilde{\theta} = \theta + \lambda, \gamma_1 \leq \tilde{\alpha} \leq \gamma_2,$

$\gamma_1 = \lambda - 0,5(\beta_{08}^{(1)} - \alpha_{08}^{(1)}), \gamma_2 = \lambda + 0,5(\beta_{08}^{(1)} - \alpha_{08}^{(1)}),$

$D_1(\alpha) = \cos^2 \alpha, D_2(\alpha) = \sin^2 \alpha.$

For specified cases of contacts:

- 1) $\varepsilon_1 = 2(\delta_1 + \delta_2), \varepsilon_2 = -(\delta_1 + \delta_2), (\delta_1 + \delta_2) < \varepsilon, a_2 < b_1$
- 2) $\varepsilon_1 = 2\delta_1, \varepsilon_2 = -\delta_1, \delta_1 < \varepsilon, R_2 < b_1$
- 3) $\varepsilon_1 = 2\delta_2, \varepsilon_2 = -\delta_2, \delta_2 < \varepsilon, a_2 < R_1.$

Contact semi-angle $\gamma = 0,5(\beta_{08}^{(1)} - \alpha_{08}^{(1)})$ is determined from equilibrium condition:

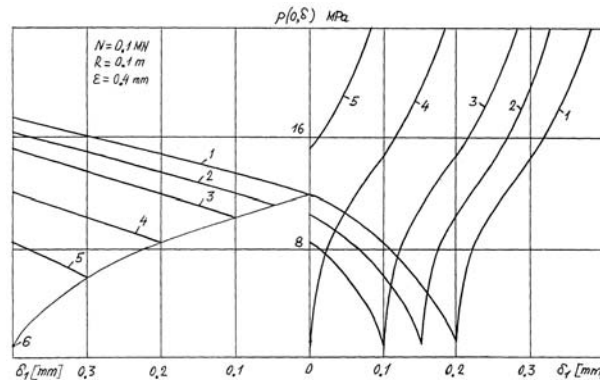


Fig.3. Plots of variations of the maximal contact pressures (uni- and bi-area contact): 1- $\delta_2=0$, 2- $\delta_2=0.05\text{mm}$, $\delta_2=0.05\text{mm}$, 3- $\delta_2=0.1\text{mm}$, 4- $\delta_2=0.2\text{mm}$, 5- $\delta_2=0.3\text{mm}$

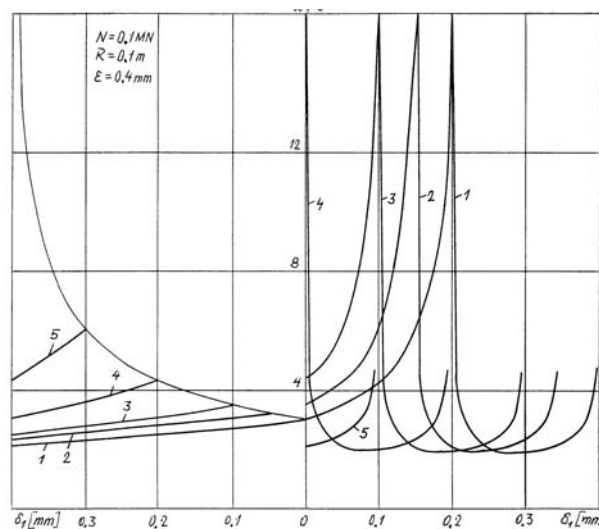


Fig.4. Plots of variations of the contact semi-angle (uni- and bi-area contact)

$$N' = R \int_{\gamma_1}^{\gamma_2} p(\tilde{\alpha}, \delta) \cos \tilde{\alpha} d\tilde{\alpha} = 2\pi R (C_0 \bar{A}_0 + C_2 \bar{A}_2) \quad (7)$$

where: $\bar{A}_0 = 1 - \tilde{b}^{-1}; \tilde{b} = \sqrt{tg^2 \frac{\gamma}{2} + 1},$

$$\bar{A}_2 = 0,5 \tilde{b}^{-1} [d_0^2 (4 - \tilde{b}) + 6(1 - \tilde{b})]; d_0 = tg \frac{\alpha_0 \delta}{2}$$

Equation (6) is solved using approximate collocation method and distribution of the contact pressures $p(\tilde{\alpha}, \delta)$ is chosen in the following form [2]:

$$p(\tilde{\alpha}, \delta) \equiv (C_0 + C_2 tg^2 \frac{\tilde{\alpha}}{2}) \sqrt{tg^2 \frac{\alpha_0 \delta}{2} - tg^2 \frac{\tilde{\alpha}}{2}} \quad (8)$$

where: C_0, C_2 - collocations coefficients.

The following data were used in calculations:
 $N = 0.1 \text{ MN}; \varepsilon = 0.4 \text{ mm}; R = 0.1 \text{ m};$ (Fig. 3 and 4).

In Fig. 3 and 4 are showed the maximal contact pressure $p(0, \delta)$ and the contact areas γ or $\alpha_{0\delta}$ (for uniarea contact) according to δ_1 and mutual orientation of elliptic contour axes. The lines on the left axis of ordinates correspond with orientation of ellipses axes showed in Fig. 1 – uniarea contact, whereas lines on the right correspond with mutual orientation of elliptic contours. The chart breaks off when $\delta_1 = \delta_2 = 0.1 \text{ mm}$ for that orientation of ellipse axes (Fig. 1) and does not occur when $0.1 \text{ mm} \geq \delta \geq 0$. The chart appears again for areas orientation showed in Fig. 1 (long axes of elliptic contours are perpendicular), but as the bi-area contact. Line 3 (Fig. 4) attains a minimum for $\delta_1 \cong 0.1 \text{ mm}$ and then grows to infinity (theoretically) because $\lambda \rightarrow \pi/2$ and $N' \rightarrow \infty$.

Plots – Fig. 4. show the angles $\alpha_{0\delta}$ and γ of uniarea and bi-area contact, respectively, according to δ_1 . One can notice that for line 3, when $p(0, \delta)$ reaches minimal value, the angle γ attains a maximum. It is predictable because applied N' acts on the larger area.

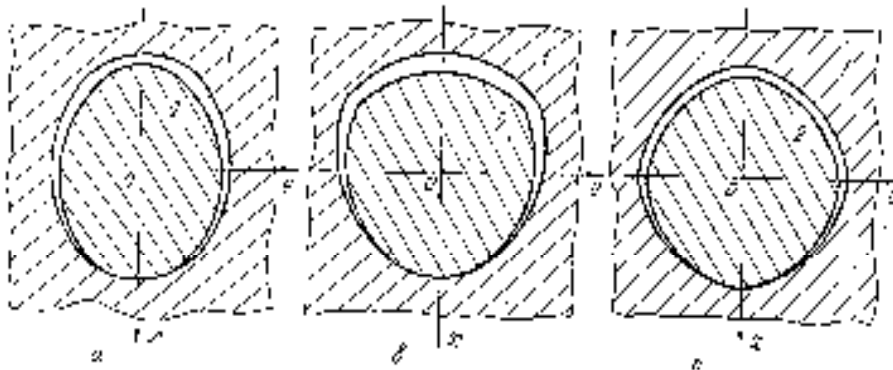


Fig. 5. Joints of lobing elements oriented symmetrically ($\delta_2 \leq \varepsilon, \delta_1 \leq \delta_2$): a) the oval disk in the oval hole, b) the trilobing disk in the trilobing hole, c) the tetralobing disk in the tetralobing hole

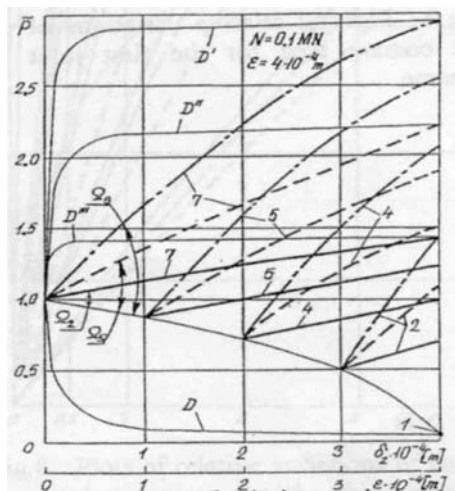


Fig. 6. Plots of relative variations of the maximal pressures for the joints showed in Fig. 5

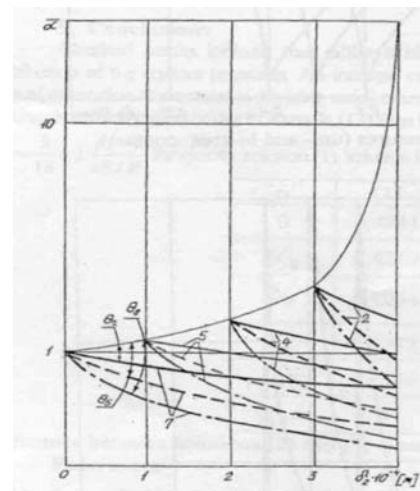


Fig. 7. Plots of relative variations of the contact area joints showed in Fig. 5

It can be said that character of charts change of the contact semi-angles γ is converse to charts $p(0, \delta)$ and minimal value of $p(0, \delta)$ corresponds with maximal value of γ .

4. Joints with lobing

Let us consider a number of element joints with the same lobing and the same orientation (Fig. 5).

Computational results are presented in the graphical way (Fig.6), where zones of \bar{p} variation for showed computational schemes are denoted by Ω_2 , Ω_3 , and Ω_8 and boundary curves for other are denoted by D' , D'' and D''' . Solid lines correspond with scheme 1 dashed with scheme 2 and dot-and-dash with scheme 3.

Where:

- scheme 1:
 $\delta_2 \leq \varepsilon, \delta_1 \leq \delta_2, D_1 = 1 + 3 \cos 2\alpha, D_2 = 1 - 3 \cos 2\alpha;$

6. References

- [1] Muscheliszwili H.M.: *Some basic problems of the theory mathematical of elasticity*. Moscow, Nauka, 1949 (in Russian, translated in English, 1953, Noordhoff, Groningen).
- [2] Panasiuk W.W., Teplýj M.J.: *Review of the contact problems in the theory of elasticity*. Kiev, Naukowa Dumka, 1975 (in Ukrainian).
- [3] Andrejkiw A.E., Czerniec M.W.: *Description of contact interaction between rubbing machine elements*, Kiev, Naukowa Dumka, 1991 (in Russian).
- [4] Person A.: *On the Stress Distribution of Cylindrical Elastic Bodies in Contact Dissertation Chalmers Tekniska Hogskola*, Goteborg 1964.
- [5] Gladwell G.: *Contact problems in the Classical Theory of Elasticity*. Alphen an den Rijn. Sijthoff and Hordhoff, 1980.

*Praca naukowa finansowana ze środków Komitetu Badań Naukowych w latach 2004-2005
jako projekt badawczy.*

- scheme 2:
 $\delta_2 \leq \varepsilon, \delta_1 \leq \delta_2, D_1 = 1 + 8 \cos 3\alpha; D_2 = 1 - 8 \cos 2\alpha;$
- scheme 3:
 $\delta_2 \leq \varepsilon, \delta_1 \leq \delta_2, D_1 = 1 + 15 \cos 4\alpha; D_2 = 1 - 15 \cos 2\alpha.$

Plots point out that more complex lobing causes an increase in the pressures at equal δ_1 i δ_2 . The greater value of δ_2 , the greater variation of the pressures occur when δ_1 i δ_2 are comparable.

Comparable values of changes of the contact areas for schemes 1,2,3 (Fig.5) are presented in Fig.7.

5. Conclusions

The plots in Fig.3 show variations of the maximal contact pressures for uni- and bi-area contact. Plots on Fig.4 show contact semi-angle $\alpha_{0\delta}$ or γ (semi- and bi-area contact) according to δ_j and mutual orientation of elliptic contour axes. On plots – Fig.4 we can notice that, when contact pressure $p(0, \delta)$ reaches minimal value, the angle γ attains a maximum.

Prof. dr hab. inż. Miron Czerniec

Instytut Technologicznych Systemów Informacyjnych
 Politechnika Lubelska
 ul. Nadbystrzycka 36, 20-618 Lublin
 e-mail: m.czerneic@pollub.pl

Dr inż. Cyprian Komorzycki

Katedra Mechaniki Stosowanej
 Politechnika Lubelska
 ul. Nadbystrzycka 36, 20-618 Lublin
 e-mail: c.komorzycki@pollub.pl
